



## Swelling and diffusion model of a hydrophilic film coating on controlled-release urea particles



Ling Yang, Di An, Ting-Jie Wang\*, Chengyou Kan, Yong Jin

Department of Chemical Engineering, Tsinghua University, Beijing 100084, China

### ARTICLE INFO

#### Article history:

Received 15 December 2015

Received in revised form 14 March 2016

Accepted 27 March 2016

Available online 20 July 2016

#### Keywords:

Coating

Controlled-release

Particle

Permeability

Swelling

Urea

### ABSTRACT

Controlled-release urea was fabricated by coating urea particles with a polymer latex in a fluidized bed. The latex film coated on the urea particle surface was hydrophilic and swelled in water. The film swelling in water and urea solution and properties of the swollen film were studied. The film swelling in urea solution followed the Lagergren's pseudo-first order kinetics with the swelling coefficient depending on the film material and experimental conditions. The effects of swelling on film structure and permeability were studied. The film permeability coefficient decreased with increasing swelling ratio with an approximately linear relationship. Based on the film formation process and structure of the swollen film, a film structure model consisting of dense and swollen phases was proposed. The permeability coefficient of the spherical film and cumulative release of urea from the coated particles were calculated from the swelling ratio of the spherical film, which was determined from the expansion curve of the coated particle during the release process. The calculated and measured release curves agreed well. This research indicates that the swelling of the hydrophilic film and the controlled-release mechanism are important factors in the development of controlled-release urea.

© 2016 Chinese Society of Particuology and Institute of Process Engineering, Chinese Academy of Sciences. Published by Elsevier B.V. All rights reserved.

### Introduction

The inefficient use of fertilizers has caused serious environmental pollution. The use of controlled-release fertilizers is an effective measure to increase their utilization efficiency and lower pollution. Controlled-release fertilizers are usually produced by coating the fertilizer particles with a synthetic polymer. Using polymer latex as a coating material, in which the continuous phase is water, and the latex is sprayed onto urea particle surfaces and forms a film after dehydration, is a promising green process for controlled-release fertilizer production (Du, Shen, & Zhou, 2013; Lan et al., 2011; Tzika, Alexandridou, & Kiparissides, 2003; Yin et al., 2015).

Unlike slow-release drugs (Dekyndt, Verin, Neut, Siepmann, & Siepmann, 2015; Li, Guo, Meng, & Zhang, 2011), controlled-release fertilizers require a long release period and low cost. Therefore, characterization of the release properties of controlled-release fertilizers is very important. Because of the long release period, measurement of their release curves usually takes tens of days or longer. Methods to shorten the measurement time have been explored; e.g., measuring the release curve in hot water or/and

at low/high pH, and then calibration with the results for release characteristics under normal conditions (Chen, Ge, Sun, Wang, & Zhang, 2012; Duan, Zhang, Liu, Yang, & Shang, 2009; Xie, Yang, Cao, Jiang, & Zhang, 2007). However, these methods could not reproduce the mechanism of the actual release process, so they usually have a large error compared with those measurements obtained under ambient conditions, and the measurement time is still long. Therefore, it is important to understand the release process and establish a release process model to allow efficient prediction of the release characteristics of controlled-release fertilizers. The effects of preparation conditions on fertilizer release properties and a release process model have been reported (Lan et al., 2013).

Film structure strongly affects the release of fertilizer particles. In the existing literature, the film structure and permeability coefficient ( $P$ ), which is defined as the permeation flux under a unit concentration gradient across the film, were assumed to be constant during the release process (Al-Zahrani, 1999; Gambash, Kochba, & Avnimelech, 1990; Shaviv, Raban, & Zaidel, 2003). Lan et al. (2013) proposed a diffusion model for film with a multi-layer and random defect structure based on the film formation process by spray coating. From the measured structural parameters and nutrient diffusion rate in this film structure model,  $P$  and the release curve of the film were calculated. The calculated release curve agreed well with that measured.

\* Corresponding author. Tel.: +86 10 62788993; fax: +86 10 62772051.

E-mail address: [wangtj@tsinghua.edu.cn](mailto:wangtj@tsinghua.edu.cn) (T.-J. Wang).

## Symbols used

$A$	permeation area of the film ( $\text{m}^2$ )
$A_s$	average surface area for single particle ( $\text{m}^2$ )
$C$	urea concentration ( $\text{g}/\text{L}$ )
$\Delta C$	concentration difference across the film ( $\text{g}/\text{L}$ )
$C_1$	low concentration of urea ( $\text{g}/\text{L}$ )
$C_2$	high concentration of urea ( $\text{g}/\text{L}$ )
$C_i$	urea concentration inside the particle ( $\text{g}/\text{L}$ )
$C_o$	urea concentration outside the particle ( $\text{g}/\text{L}$ )
$C_s$	urea concentration of saturated solution ( $\text{g}/\text{L}$ )
$C_w$	urea concentration in the water tube ( $\text{g}/\text{L}$ )
$J$	permeation flux ( $\text{g}/(\text{m}^2 \text{s})$ )
$k$	swelling coefficient ( $\text{s}^{-1}$ )
$\Delta m$	penetration amount of urea through the film (g)
$m_0$	initial mass of coated urea in the release process (g)
$m_L$	coating amount of latex on a single urea particle (g)
$M_0$	mass of the urea solution outside of the particles in the vessel (g)
$m_s$	urea mass in a single coated urea particle (g)
$N$	number of particles
$P$	permeability coefficient of the film ( $\text{m}^2/\text{s}$ )
$P_0$	permeability coefficient for unswollen film ( $\text{m}^2/\text{s}$ )
$P_a$	apparent permeability coefficient ( $\text{m}^2/\text{s}$ )
$P_x$	permeability coefficient of the infinitesimal cross-section ( $\text{m}^2/\text{s}$ )
$R^2$	correlation coefficient
$R_{ac}$	accumulated quantity released from a single particle (%)
$t$	time (s)
$\Delta t$	time interval in measurement (s)
$V$	total volume of the expanded particles ( $\text{m}^3$ )
$V_s$	volume of a single particle ( $\text{m}^3$ )
$W$	mass of the swollen spherical film (g)
$W_0$	dehydrated mass of the swollen spherical film (g)
$w_i$	mass of the $i$ th plane film (g)

### Greek letters

$\alpha$	fitted parameter (%)
$\beta$	fitted parameter (%)
$\gamma$	fitted parameter ( $\text{L}/\text{g}$ )
$\delta$	film thickness (m)
$dx$	thickness of infinitesimal cross-section (m)
$\eta$	impact factor of swelling ( $\text{m}^2/\text{s}$ )
$\rho$	density of the swollen film ( $\text{g}/\text{L}$ )
$\Phi$	swelling ratio of the spherical film (%)
$\varphi_e$	equilibrium swelling ratio (%)
$\varphi_i$	swelling ratio of the $i$ th plane film (%)

Latex films formed from the dehydration of atomized droplets on the surface of fertilizer particles are hydrophilic (Lan, 2012), so such films swell markedly in water. The swelling properties of hydrophilic polymers have been widely studied. Tanaka and Fillmore (1979) used a displacement vector to describe the swelling process of spherical gel particles in water, finding that the displacement of a gel network point depended on swelling time and location. Li and Tanaka (1990) investigated an infinite planar film and reported that the swelling displacement curve of the network increased exponentially. Kostic, Adnadjevic, Popovic, and Jovanovic (2007) proposed that the swelling rate and equilibrium swelling ratio ( $\varphi_e$ ) of poly(acrylic acid) gel were higher in pure water than normal saline solution because of ionic osmotic pressure. The

swelling ratio of polyacrylamide gel changed exponentially with time in NaCl solution at low concentration (Sivanantham & Tata, 2012). Ataman and Pekcan (2007) calculated  $P$  of small molecules in a swollen iota-carrageenan using Fick's law and the Li-Tanaka model (Li & Tanaka, 1990). The calculated activation energies of diffusion and swelling were 20.5 and 28.2 kJ/mol, respectively. Lang, John, and Sommer (2016) studied the network formation and swelling of a cross-linking co-polymer and found the swelling data of most networks agreed with the prediction of the Flory-Rehner model. An additional non-affine contribution to the equilibrium degree of swelling was observed for networks with a low density of active cross-links.

The swelling of a hydrophilic film changes its structure, which changes its nutrient  $P$ . The effects of swelling on  $P$  have been examined. Yakimets et al. (2007) studied the water uptake of three types of biopolymer films and found that the structural reorganization and elastic properties of the films depended on water content. Zhu and Vesely (2007) reported that swelling has a marked effect on the diffusion and permeation rates of methanol in a polymethylmethacrylate film, and that  $P$  can be modified by controlling the swelling ratio. Kim et al. (2009) controlled the release rate of a drug in a capsule by controlling swelling and deswelling. The drug was released very slowly or not at all in pure methanol because the coated film was not swollen. When the capsule was immersed in aqueous methanol with 90% (v/v) water, the drug release rate was fast because of the swelling of the film. When the capsule was reimmersed in methanol, drug release became slow again. Other researchers have also reported that film swelling caused by hydrophilicity accelerated the release rate of particles (Kurek, Guinault, Voilley, Galic, & Debeaufort, 2014). Fan et al. (2008) reported that film swelling and drug permeability were consistently related.

This paper studies the swelling properties and process of a hydrophilic film, and the relationship between the swelling ratio and film permeability. A structure model of the swollen film and a release process model are established to predict the release characteristics of film-coated urea particles.

## Experimental

### Materials and instruments

Large granular urea with a diameter of 2–3.2 mm (China Blue Chemical Ltd., Beijing, China) was coated with styrene-butyl acrylate copolymer latex with 40% solid content. The latex nanoparticles had an average diameter of 80 nm (Li, Kan, & Liu, 2001) and were synthesized by semi-continuous emulsion copolymerization of butyl acrylate, styrene, methacrylic acid, and crosslinker (Lan et al., 2013). The other chemicals used were urea, ethanol, and hydrochloric acid (analytical grade, Beijing Modern Oriental Fine Chemicals Co., Ltd., Beijing, China), 4-dimethylaminobenzaldehyde (DMAB; analytical grade, Sinopharm Chemical Reagent Co., Ltd., Shanghai, China), and deionized water.

The film structure was characterized by a high-resolution scanning electron microscope (SEM, JSM7401, JEOL, Tokyo, Japan). An ultraviolet-visible spectrophotometer (TU-1900, Beijing Purkinje General Instrument Co., Ltd., Beijing, China) was used to measure the concentration of the urea solution. A precision balance (0.1 mg, PWC214, Adam Equipment Co., Ltd., Milton Keynes, UK) was used to measure the mass of the swollen film. An oven (101-2AB, Beijing Zhongxing Weiye Instrument Co., Ltd., Beijing, China) was used for dehydration and heat treatment of the planar film. A micrometer (0–25 mm, Beijing Blue Light Group, Beijing, China) was used to measure film thickness.

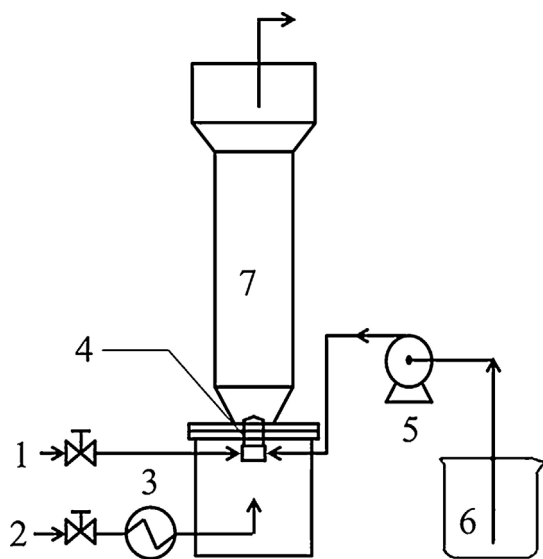


**Fig. 1.** Schematic diagram of the experimental apparatus used to coat urea particles. 1: atomizing gas; 2: fluidization gas; 3: heater; 4: nozzle; 5: peristaltic pump; 6: styrene-butyl acrylate latex; 7: fluidized bed.

#### Preparation of the planar film and coated urea particles

The planar film was prepared as follows. A 150 mm × 200 mm rectangular area of a glass sheet was surrounded by medical tape with a thickness of 280 µm. Latex diluted to a solid content of 30% was dropped onto the center of the rectangular area. A planar layer of latex was produced by brushing the latex solution with a glass rod. The latex layer on the glass sheet was dehydrated in an oven at 80 °C for 30 min and then thermally treated at 120 °C for 1 h to remove residual water and increase polymer cross-linking in the film. The resulting planar film with uniform thickness was cooled to room temperature and removed from the glass sheet for subsequent examination.

Urea particles were coated in a fluidized bed (Fig. 1), which was made of stainless steel with an external thermal isolation layer. The fluidized bed had an inner diameter of 150 mm and height of 900 mm. The bottom of the bed was tapered and the top was expanded to avoid particles being entrained. After the fluidization gas was heated to the set temperature, granular urea (1 kg) was put into the fluidized bed. Latex with a set solid content was pumped into a nozzle and atomized by the atomization gas at a set flow rate. The atomized droplets with an average size of 50 µm were coated on the surface of the urea particles in the fluidized bed. The droplets spread out, were dehydrated and formed a film. The film coating process was random, intermittent, and repeated. Film thickness was controlled by adjusting the coating amount. The coated urea was thermally treated at the high temperature of the fluidizing gas for 30 min to remove the remaining moisture in the film and increase the cross-linking degree of the polymer. The coated urea particles were cooled with fluidization gas to room temperature before measurement of their release rate.

#### Characterization of film swelling

##### Planar film swelling in water and urea solution

Circular films (60-mm diameter) were used to examine the planar film swelling in water and urea solution. A saturated urea solution was first prepared and then used to produce urea solutions with volume concentrations that were 0%, 10%, 20%, 40%, 60%, 80%, and 100% of the saturated concentration. The concentration of the saturated urea solution was measured to be 620.9 g/L at 25 °C. Seven

sheets of film of weighed mass  $w_i$  ( $i = 1-7$ ) were put in the urea solutions at 25 °C. After a set time, the seven sheets were taken out and the water on each film surface was removed using absorbent paper. The swollen films were weighed as  $w_i(t)$  ( $i = 1-7$ ). The swollen films were put back in each solution for further swelling and subsequent measurement. Parallel experiments were conducted, and the average of the two measured values was used for each film. Experiments displayed excellent repeatability. The swelling ratio of each film in urea solution at time  $t$ ,  $\varphi_i(t)$ , was obtained as

$$\varphi_i(t) = \frac{w_i(t) - w_i}{w_i} \times 100\%, \quad i = 1, 2, \dots, 7. \quad (1)$$

##### Spherical film swelling during the release process

Eight samples of coated urea particles were prepared to measure how the spherical film swelling ratio changed with time. Coated urea particles (10 g) were put in a nylon mesh bag. The bag was placed in a bottle containing deionized water (0.2 kg). The urea particles in the bag were not squeezed in the water. The solution in each bottle was replaced with fresh deionized water (0.2 kg) every 48 h. A particle sample was taken out every 6 days during the release process. Spherical films of the sample particles were obtained by cutting the coated particles of each sample and washing them with deionized water to remove the urea on the film surface. The water on the spherical film surface was removed using absorbent paper. The swollen films were weighed as  $W(t)$ . The swollen films were then dehydrated in an oven at 80 °C for 1 h and the dehydrated films were weighed as  $W_0$ . The swelling ratio of the spherical film at time  $t$ ,  $\Phi(t)$ , was obtained using Eq. (1).

##### Microstructure of the swollen films

To examine the structure of the swollen films, the film structure was visualized as follows. A sheet of circular planar film with a diameter of 40 mm was fixed in a U-shaped tube apparatus with flanges and rubber gasket (Fig. 2). Both sides of the U-shaped tube were kept at the same height as the initial liquid levels. Film swelling was conducted under two configurations: (1) deionized water on both sides, and (2) saturated urea solution on one side and deionized water on the other. The solutions on both sides were changed every two days. To ensure the films reached swelling equilibrium, the immersion time was 100 days. The swollen films were taken out and water on each film surface was removed with absorbent paper. The swollen films were immediately put into liquid nitrogen for 1 min to obtain film sections following freezing and cleavage (Aranaz, Gutierrez, Ferrer, & del Monte, 2014). The microstructure of film sections was examined by SEM.

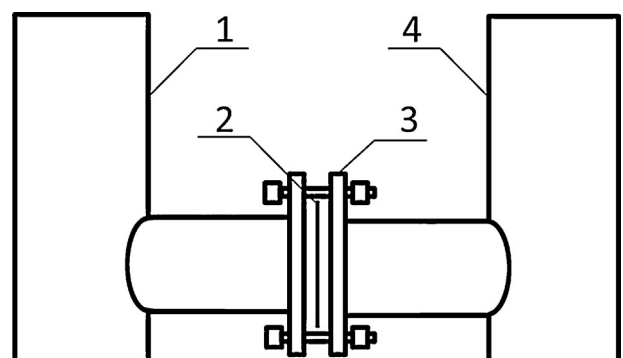
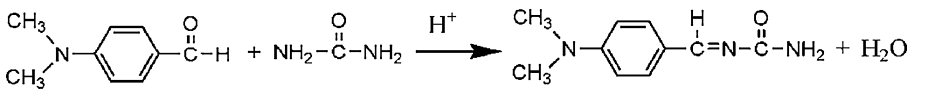


**Fig. 2.** Schematic diagram of the U-shaped tube apparatus. 1: urea saturated solution/deionized water; 2: planar film; 3: flange; 4: deionized water.

### Determination of film permeability

Urea solution concentration was measured as follows. Hydrochloric acid (35%) was added to ethanol with a 1:10 volume ratio, then DMAB was added to the mixed solution. Under acidic conditions, DMAB and urea reacted to produce (4-dimethylamino-benzylidene)-urea, which is yellow. The higher the concentration of this product, the deeper the yellow of the solution. The reaction of DMAB and urea is shown in Eq. (2). The product has a characteristic absorption peak at 430 nm, where neither DMAB nor urea absorbs. Therefore, the product can be quantified by the absorbance at 430 nm. In the concentration range used, the concentration and absorbance of the solution follow the Beer-Lambert law; i.e., the concentration and absorbance have a linear relationship. Thus, the urea concentration can be determined by measuring the absorbance of the solution at 430 nm and calibration (Lan, 2012).



### Determination of planar film permeability

Fig. 2 shows the U-shaped tube apparatus used to measure  $P$  of the planar films. A film with a diameter of 40 mm was fixed in the connection center of the U-shaped tube. The left side of the U-shaped tube was filled with saturated urea solution and the right with deionized water. The initial levels of the solutions in both tubes were maintained at the same height. After time  $\Delta t$ , the solution on the right was taken out, and the volume and urea concentration of the sampled solution were measured. The penetration amount of urea  $\Delta m$  was calculated from the volume and urea concentration of the solution sampled from the right tube. The measurements showed that the  $P$  was usually very small for a dense film and the urea concentration  $C_w$  of the solution on the right was very low. Therefore, the concentration difference across the film was  $\Delta C = C_s - C_w \approx C_s$ , where  $C_s$  is the concentration of saturated urea solution. Using Fick's first law,  $P$  of the planar film was calculated by Eq. (3) (Lan et al., 2011). There was no obvious film deformation during the measurement, so it was assumed there was no change of film permeation area or thickness. Measurements were repeated to verify the reproducibility of the permeability measurement, and the average of the two measured values was used.

$$J = P \frac{\Delta C}{\delta} = \frac{\Delta m}{A \Delta t} \rightarrow P = \frac{\delta \Delta m / \Delta t}{C_s A}, \quad (3)$$

where  $J$  is permeation flux,  $\delta$  is the film thickness measured by a micrometer, and  $A$  is film permeation area.

### Determination of spherical film permeability

During the release of urea from the coated urea particles in water, the concentration difference across the film varied, so the surface area of the spherical film also varied because of film swelling and the volume expansion of the coated particles. Therefore, the permeability of urea via the film was measured. Coated urea particles (~50 g) were weighed accurately as  $m_0$  and placed in a nylon mesh bag. The coated urea particles were put into a bottle of deionized water (1 kg). The urea particles were not squeezed, but they did stack because of their slight gravity in water. During the release process, urea was released slowly through the film, and water outside the film also diffused inside the particles. No film rupture was observed. To measure the release rate, the mass of water entering the particle interior and the mass of released urea were measured. This allowed the urea concentration in the particle, surface area of the film, film thickness, and other parameters and their changes with release time to be calculated. To measure the release rate

and urea concentration accurately, the solution was taken out and replaced with fresh deionized water (1 kg) every 48 h so that the coated particles continued to release urea freely. The replaced solution was weighed and its urea concentration was measured.

From the mass  $M_0(t)$  and concentration  $C_0(t)$  of the urea solution, the mass of urea released  $\Delta m(t)$  was determined, and the total volume of the expanded urea particles  $V(t)$  during release was calculated. Combining  $V(t)$  with the number of particles  $N$  in the mesh bag, the average volume  $V_s(t)$  and surface area  $A_s(t)$  of a single particle and spherical film thickness of the particles  $\delta(t)$  were obtained. The average of the two values measured in parallel was used, and the values showed good repeatability. Using Fick's first law, the time-dependent permeability coefficient  $P(t)$  of a spherical film was calculated as

$$P(t) = \frac{\delta(t) \Delta m(t) / \Delta t}{N[C_i(t) - C_o(t)]A_s(t)}, \quad (4)$$

where  $C_i(t)$  and  $C_o(t)$  are the urea concentration inside and outside the particle, respectively.

## Results and discussion

### Dense film formation by spray coating

A film was prepared using latex with 40% solid fraction by filtration through double-layer membranes with pores with an average diameter of 0.22  $\mu\text{m}$  and subsequently dehydrated (Fig. 3(a)). The film consisted of closely packed latex particles, and there were dense tiny pores between the particles. When the film was thermally treated in an oven at 80 °C for further dehydration, the film became denser. Fig. 3(b) shows the film surface morphology of the filtered latex after drying at 80 °C for 15 min. The particles in the film fused with each other to form a continuous uniform film. Fig. 3(c) depicts a cross section of the planar film formed by spray coating and thermal treatment at 120 °C for 30 min, indicating a uniform dense structure. The coated urea particles in the fluidized bed also possessed a dense film of uniform thickness. The spherical film had no visible defects, indicating good contact between it and the urea (Fig. 3(d)).

The dehydration process strongly affected the film formation process. As the latex particles got closer to each other during dehydration, the dehydration rate gradually decreased. When the dehydration temperature was higher than the minimum film formation temperature of the latex (25 °C), the latex particles began to deform irreversibly. They changed from spherical to polyhedral because of the capillary force, but an interface remained between particles. As the thermal treatment process continued, residual water diffused out from the film surface through the channels between the particles, and the polymer chains twisted and entangled with each other. As the latex particles melted further, the polymer chains cross-linked to form a network structure, eventually forming a film with high mechanical strength.

### Swelling kinetics of the hydrophilic film in urea solution

Because the film molecules have hydrophilic groups such as carboxylate ( $-\text{COO}^-$ ), ester ( $-\text{COOR}$ ), and amide ( $-\text{CONH}-$ ) moieties, when the film was immersed in water, water molecules diffused into the film and formed hydrogen bonds with the hydrophilic groups, causing the film to swell. There are many reports on gel swelling kinetics (Alfrey, Gurnee, & Lloyd, 1966; Crank, 1975; Li &

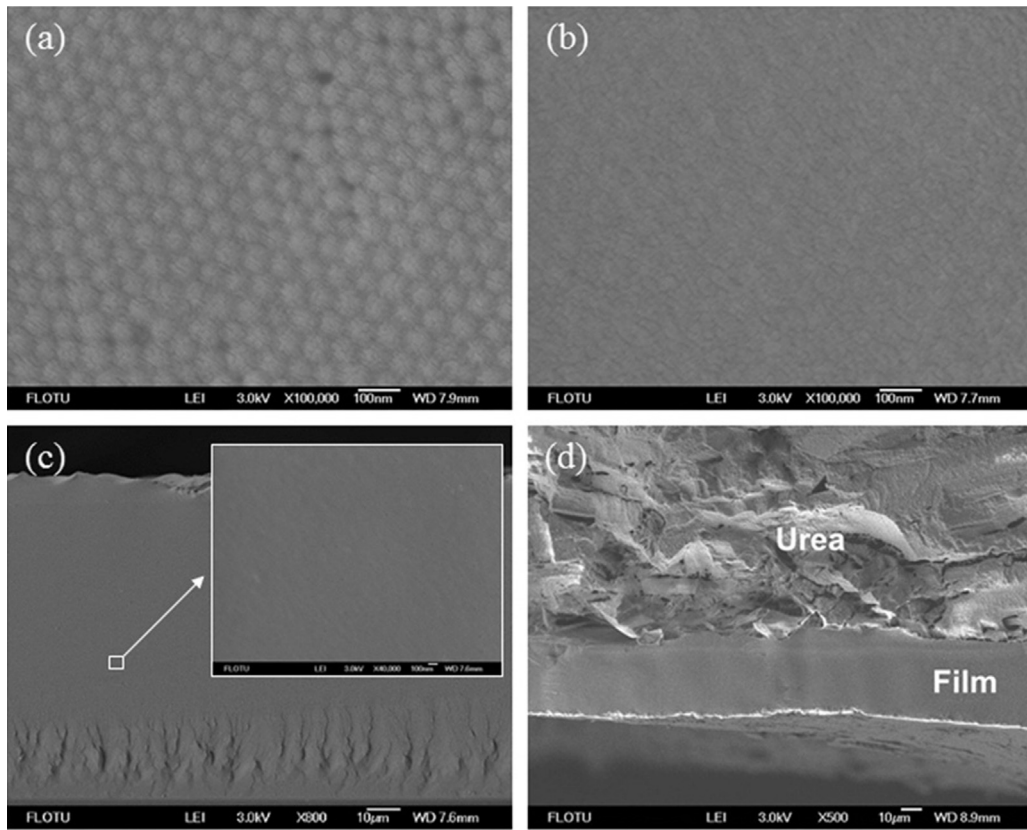


**Fig. 3.** Surface and cross-sectional structure of the latex film under different conditions. (a) Surface of filtered latex, (b) film surface of filtered latex after it was dried at 80 °C for 15 min, (c) cross-section of the planar film obtained by spray coating after thermal treatment at 120 °C for 30 min, and (d) cross-section of a spherical film after thermal treatment at 120 °C for 30 min.

Tanaka, 1990; Schott, 1992; Wang, Li, & Hu, 1997). The swelling kinetics model based on Fick's first law (Alfrey et al., 1966; Crank, 1975) describes the swelling process as: (1) water molecules diffuse into the polymer network; (2) the polymer chains become hydrated, causing them to relax; (3) the polymer chains diffuse into the surrounding space, and when the forces between the volume expansion caused by the diffusion of the polymer chains and the elastic shrinkage of the molecular chain network reach equilibrium, the swelling reaches equilibrium. According to this swelling kinetics model, water molecule diffusion is the rate-determining step for hydrogel swelling. The number of active sites in a polymer latex film that can form hydrogen bonds with water molecules is usually much lower than that in a hydrogel, and the elastic shrinkage of a latex film caused by its polymer network is usually much stronger than that of a hydrogel. Therefore,  $\varphi_e$  of a latex film is much lower than that of a hydrogel. That is,  $\varphi_e$  of the latex film in this paper reached a maximum of 100%, as illustrated in Fig. 4 (marked as "0% sat" curve; i.e., 0% of the saturation concentration), while  $\varphi_e$  of a hydrogel is usually over 1000% (Witono, Noordergraaf, Heeres, & Janssen, 2014). This indicates that the interaction between water molecules and the polymer chain is the main factor dominating the swelling process of the latex film.

Water molecules form hydrogen bonds with the hydrophilic groups in the polymer. The water molecules are held between the polymer chains, similar to molecule/ion adsorption on a solid surface in a solution. Using the Lagergren kinetic equation for a liquid–solid adsorption process, which is a pseudo-first-order adsorption equation (Ho, 2004), in the swelling process, the site that forms a hydrogen bond with a water molecule is regarded as the active site. Water molecules that collide with an empty active site are held in the polymer, so the concentration of empty active

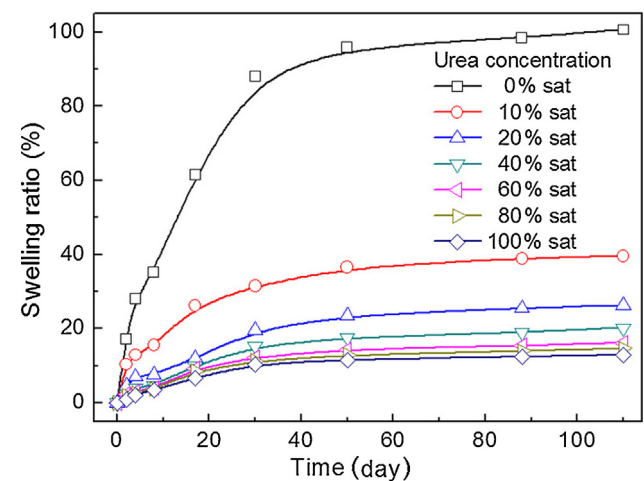


**Fig. 4.** Film swelling ratios as a function of time in urea solutions of different concentrations.

sites is taken as the driving force of swelling. The swelling rate can be expressed as,

$$\frac{d\varphi}{dt} = k(\varphi_e - \varphi), \quad (5)$$

where  $\varphi$  is the swelling ratio at time  $t$ ,  $(\varphi_e - \varphi)$  is the driving force, and  $k$  is the swelling coefficient, which depends on the film material and experimental conditions. A larger  $k$  indicates a higher swelling

rate. Combined with the initial condition  $t=0, \varphi=0$ , the swelling kinetic equation can be expressed as,

$$\varphi = \varphi_e(1 - e^{-kt}). \quad (6)$$

The swelling curve of the film in deionized water is the curve labeled “0% sat” in Fig. 4.  $\varphi$  increased exponentially over time. The swelling curves of films in urea solutions with different concentrations were measured (Fig. 4). These curves showed that the concentration of the urea solution has a considerable effect on film swelling. This is because different  $\varphi$  values reflect different hydration states. In deionized water,  $\varphi_e$  of the film was about 100%, while in urea solution that was 10% of the saturated concentration,  $\varphi_e$  was only 40%. In the saturated urea solution,  $\varphi_e$  was only 12%, which was much smaller than that in deionized water. Therefore, for a specified material and swelling conditions,  $\varphi_e$  of the film is a function of urea concentration; i.e.,  $\varphi_e(C)$ . A higher concentration of the urea solution gives a lower  $\varphi_e$ .

In urea solution, urea and water easily form hydrogen bonds, which lower the mobility of water molecules. Meanwhile, urea limits the formation of hydrogen bonds between the polymer chains and water molecules by forming hydrogen bonds with water (Cai, Liu, & Liang, 2012; Carr, Buchanan, Schmidt, Zanni, & Skinner, 2013; Rezus & Bakker, 2006; Zou, Habermann-Röttinghaus, & Murphy, 1998), which weakens the film swelling. In urea solution of low concentration, the bonding of water molecules to urea is relatively weak, so the water molecules have high mobility, and water and polymer form more hydrogen bonds, leading to a high swelling degree of the film. In a urea solution of high concentration, the bonding of water molecules to urea is strong, so water molecules have low mobility, and water and polymer form few hydrogen bonds, and the swelling degree of the film is low.

According to the measurement results for different urea concentrations,  $\varphi_e$  of the latex film in urea solution is,

$$\varphi_e(C) = (\alpha + \beta e^{-\gamma C})(1 - e^{-kt}), \quad (7)$$

where parameters  $\alpha$ ,  $\beta$ , and  $\gamma$  are determined by fitting Eq. (7) to the experimental data. From Eqs. (6) and (7), the kinetic equation of the swelling in urea solution is obtained as

$$\varphi(C, t) = (\alpha + \beta e^{-\gamma C})(1 - e^{-kt}). \quad (8)$$

Through curve fitting to the experimental data points, the parameters in Eqs. (7) and (8) were obtained, giving  $k=0.0612$ ,  $\alpha=14.8$ ,  $\beta=85.5$ ,  $\gamma=0.119$ ,  $R^2=0.990$ . The experimental and fitting results are presented in Fig. 5. The fitted curves agree well with the experimental results.

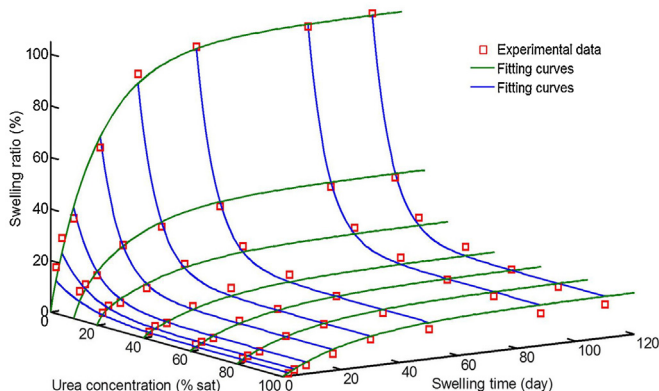


Fig. 5. Experimental results and fitted curves of film swelling in urea solution.

### Structure of the swollen film

#### Effects of urea on the swollen film structure

The cross-linking degree of the polymer affects the film swelling. A highly cross-linked film has a compact structure, so it swells slowly and its  $k$  is small. The swelling changes the film structure, which affects  $P$ . To examine the effects of swelling on the film structure, the swollen film was rapidly frozen in liquid nitrogen to convert the water molecules in the film to small ice crystals. After the sublimation of the ice crystals, a porous structure formed in the film (Aranaz et al., 2014). The size, density, and amount of pores reflect the water distribution in the film. Fig. 6 shows cross sections of the swollen films under different swelling conditions after rapid freezing in liquid nitrogen. Fig. 6(a) is the cross section of the film swelled in deionized water at equilibrium swelling. The film contained dense pores that were distributed evenly, and had a large average size of 0.5 μm, reflecting the water distribution in the swollen film. Fig. 6(b) displays the cross section of the swollen film at equilibrium swelling when one side was deionized water and the other was a saturated solution of urea. The side exposed to deionized water has a porous structure similar to that in Fig. 6(a), and the side exposed to saturated urea solution has a dense structure. This means there is a structure transition from the porous structure on the side with deionized water to the dense structure on the side with the saturated urea solution. The places where there are many large pores in the swollen film have a high water content, and places where there are few small pores (dense structure) have low or no water content. Film swelling was strongly suppressed on the side of the saturated urea solution. The results in Fig. 6 are consistent with the measured quantitative results in Fig. 4. For the side exposed to deionized water, water diffused easily into the polymer network of the film, causing considerable swelling. For the side exposed to the saturated urea solution, hardly any water diffused into the polymer network, and the swelling was limited.

#### Structure model of the swollen film

Non-uniform two-phase structures consisting of dense and dilute phases in swollen polymers have been reported (Geissler, Hecht, & Duplessix, 1982; McCoy & Muthukumar, 2010). The dense phase consists of polymer with a low water content. The dilute phase has a high water content. In the rapid freezing process, the water molecules freeze and form a porous structure after vacuum dehydration or sublimation (Fig. 6).

Considering that the swollen film consisted of uneven dense and dilute phases, it was assumed that the film consisted of a dot matrix of dense phase surrounded by the swollen phases. The diffusion of urea molecules in the film occurred in two ways: through the dense phase, which had a high resistance to urea diffusion resulting in a very low diffusion rate, and through the “channel” (swollen phase) between dense-phase dots. Although the polymer chains between the dense-phase dots had good fusion, cross-linking and winding, the diffusion resistance to urea molecules was lower there than that in the dense phase. Therefore, it was assumed that urea molecules mainly diffused through the swollen phase during mass transfer. When water molecules diffused into the dense-phase and caused the film to swell, the diffusion channel of the swollen phase was narrowed because of the dot expansion. This increased diffusion resistance, decreasing the urea diffusion rate in the swollen film.

Fig. 7 is a schematic diagram of the film cross-section showing urea diffusion. On the left of the film is urea solution of high concentration and on the right is a low-concentration urea solution. Because of the concentration difference between the two sides of the film, gradients of the swelling, urea concentration, and  $P$  are formed across the film. The apparent permeability  $P_a$  is the integrated average of  $P$  across the film.

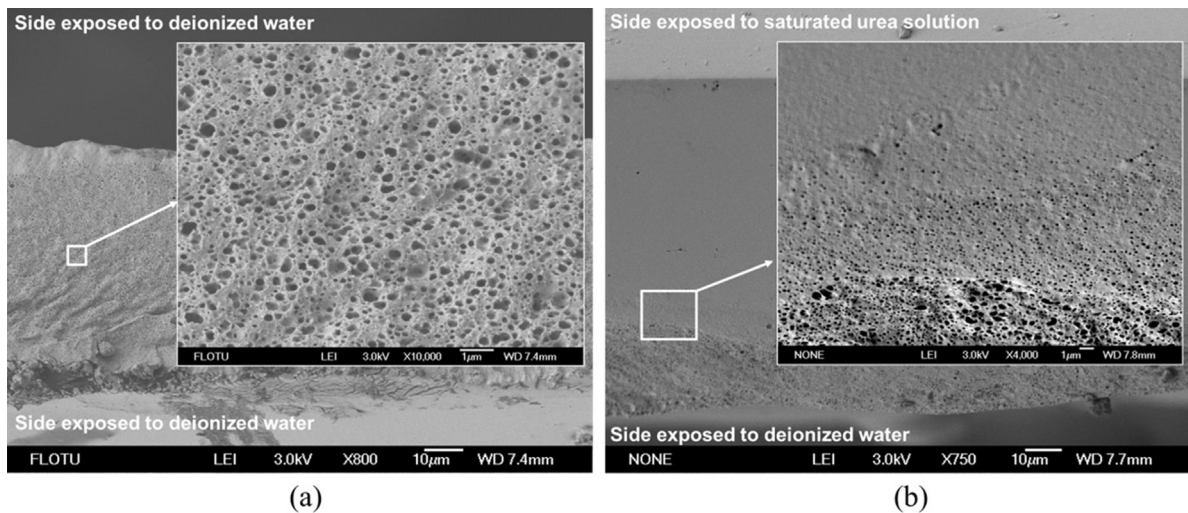


**Fig. 6.** SEM images of cross sections of a swollen film after rapid freezing in liquid nitrogen when (a) both sides of the film were exposed to deionized water, and (b) one side of the film was exposed to deionized water and the other to a saturated aqueous solution of urea.

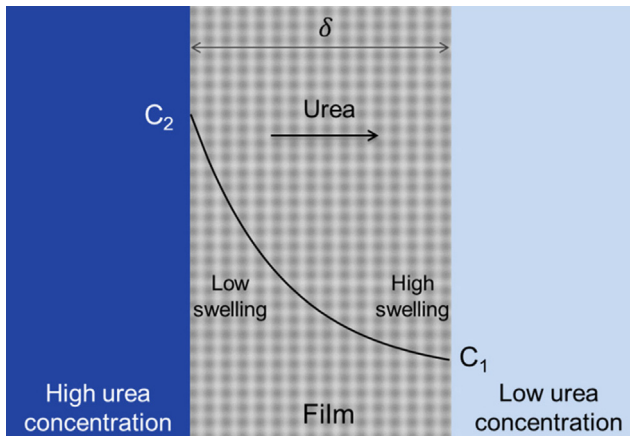


**Fig. 7.** Schematic diagram of the two-phase structure and release process in the swollen film.

#### Permeability coefficient of the swollen film

##### Measured permeability coefficient of the swollen film

The change in film structure induced by swelling affected  $P$ . Experiments were conducted to investigate the effect of swelling on  $P$ . Films with different swelling degree were prepared by immersing 14 planar films in deionized water for different periods. The  $P$  values of the films with different swelling degrees were measured using the U-shaped tube in Fig. 2. To ensure the accuracy of the measurements, measurements were conducted using two different films swollen to the same degree. The average of the two values was taken as the  $P$  of the swollen films. Fig. 8 shows  $\varphi$  and  $P$  of the films versus swelling time.  $\varphi$  increased with swelling time until reaching equilibrium swelling, while  $P$  decreased with swelling time until it gradually became constant. A low  $\varphi$  correlated with a high  $P$ . When the swelling was near equilibrium swelling,  $P$  became constant. From Fig. 8, the relationship between  $P$  and  $\varphi$  of the planar film in water was obtained, which is illustrated in Fig. 9. The relationship of  $P$  with  $\varphi$  for the planar film was linearly fitted as

$$P = \eta\varphi + P_0, \quad (9)$$

where  $\eta$  is the impact factor of swelling (a higher  $\eta$  means swelling has a larger effect on  $P$ ), and  $P_0$  is the permeability coefficient when  $\varphi = 0$ . After optimized fitting,  $\eta = -13.9 \times 10^{-15} \text{ m}^2/\text{s}$ ,  $P_0 = 15.8 \times 10^{-15} \text{ m}^2/\text{s}$ , and  $R^2 = 0.919$ .

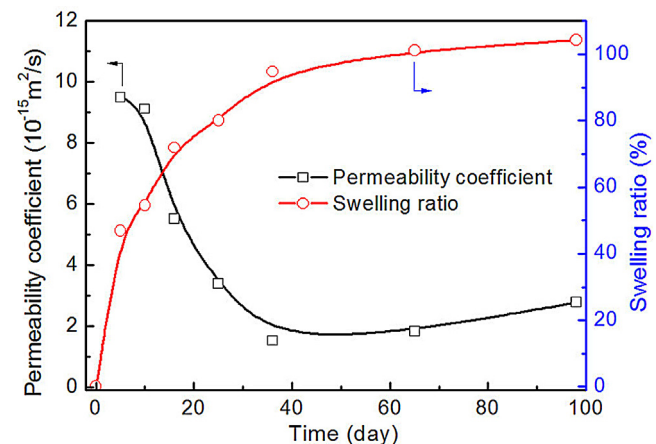


**Fig. 8.** Variations of swelling ratio and permeability coefficient of the planar film with swelling time.

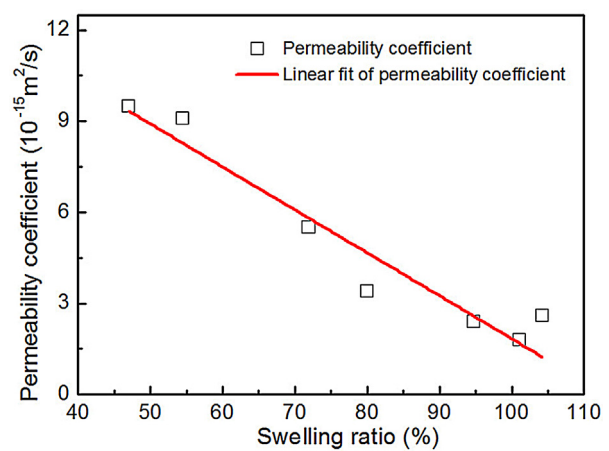


**Fig. 9.** Dependence of the permeability coefficient of the planar film on swelling ratio.

##### Permeability coefficient calculated from the structure model of the swollen film

By substituting Eq. (8) into Eq. (9), the permeability coefficient of the film in urea solution at concentration  $C$  and swelling time  $t$ ,  $P(C,t)$ , is

$$P(C, t) = \eta \varphi_e(C)(1 - e^{-kt}) + P_0. \quad (10)$$

Because urea diffusion was very slow in the film, it was assumed that the mass transfer process was at quasi-steady state. For an infinitesimal thickness of cross-section  $dx$  in the film, the mass transfer flux is the same in every infinitesimal cross-section, so Eq. (3) gives

$$\frac{\Delta m}{At} = \frac{P_a \Delta C}{\delta} = \frac{P_x dC}{dx}, \quad (11)$$

where  $\Delta m$  is the urea penetration amount of through the film,  $A$  is the film area,  $t$  is the mass transfer time,  $\delta$  is the film thickness, and  $P_x$  is the permeability coefficient of the infinitesimal cross-section  $dx$ . From Eq. (11),

$$\frac{P_a \Delta C}{\delta} dx = P_x dC. \quad (12)$$

Therefore,  $P_a$ , the apparent film permeability coefficient in the urea diffusing direction, can be expressed as

$$P_a(t) = \frac{\int_{C_1}^{C_2} P_x dC}{\Delta C}. \quad (13)$$

Substituting Eq. (10) and integrating Eq. (13) yield,

$$P_a(t) = \eta \left( \alpha + \frac{\beta}{\gamma \Delta C} e^{-\gamma C_1} - \frac{\beta}{\gamma \Delta C} e^{-\gamma C_2} \right) (1 - e^{-kt}) + P_0. \quad (14)$$

In the urea release process,  $C_1$  is usually much lower than  $C_2$ , so it was assumed  $C_1 = 0$  and the driving force is  $\Delta C = C_2 - C_1 \approx C_2$ . Eq. (14) is then simplified to

$$P_a(t) = \eta \left( \alpha + \frac{\beta}{\gamma C_2} - \frac{\beta}{\gamma C_2} e^{-\gamma C_2} \right) (1 - e^{-kt}) + P_0. \quad (15)$$

According to Eq. (15),  $P_a$  of the planar film in urea solution varies with  $C$  and  $t$  (Fig. 10). After a long  $t$ ,  $C$  and  $P$  are both low. This is because a longer  $t$  and lower  $C$  result in a higher  $\varphi$  of the film. Thus, the structure of the film changes to a greater extent, so swelling has a larger effect on  $P$ .

#### Verification of the release model of the swollen film

Distinct from the reported release model (Shaviv et al., 2003), the urea release curve can be calculated from the expansion curve of the urea particles by combining the swelling kinetics and  $P$  of the swollen film. When the coated urea particles have no expansion, the urea release rate can be directly calculated from the swelling

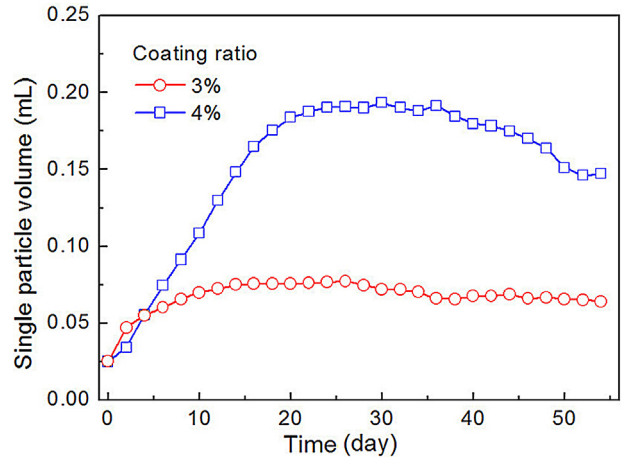


**Fig. 11.** Measured volume expansion of coated urea particles during the release process.

properties of the film material and the relationship between  $P$  and  $\varphi$ . This is much simpler than performing measurements. The urea release curve is the main characteristic used to evaluate the controlled release of urea. To verify the release model, coated urea particles with film coating contents of 3% and 4% were prepared and their release curves measured. The release characteristics of the coated urea particles were also calculated using the release model.

#### Expansion of the coated urea particles

When the coated urea particles were immersed in water, water diffused inside the spherical film. Thus the urea dissolved and was released. The difference in urea concentration between inside and outside the film produced an osmotic pressure inside the film, leading to particle expansion and film creep. During the expansion of the particles, the thickness and surface area of the spherical film changed. Fig. 11 plots the average volume of the particles against release time in water. The maximum volume reached was about 8 times the initial volume.

#### Permeability coefficient of the spherical film

During the release process of the coated urea particles, the difference in urea concentration between inside and outside the film decreased because the urea concentration inside the film decreased. In addition, the particle volume expanded because of the osmotic pressure generated by the difference in urea concentration between inside and outside the film. The osmotic pressure produced a creep stress in the film, which made its swelling more complicated. To simplify the calculation of  $\varphi$ , the effect of osmotic pressure on swelling was ignored. Because the film material and experimental conditions were not changed, the driving force for spherical film swelling in urea solution was the difference between  $\varphi_e$  and  $\varphi$ . From Eq. (5), for the spherical film this was assumed to be

$$\frac{1}{\varphi_e(C) - \varphi(C, t)} \frac{\partial \Phi(C, t)}{\partial t} = k, \quad (16)$$

where  $k$  depends on the film material and experimental parameters of the swelling like temperature and pH. Here,  $C$  is the equivalent concentration of urea in the film, which was taken to be the arithmetic mean concentration of inside and outside the film. Because the urea concentration outside the coated particles,  $C_0$ , was approximately zero, and the concentration in the coated particle was  $C_i$ ,  $C$  of the spherical film was taken to be  $C = C_i/2$ . To determine  $C_i$ , the concentration of urea solution in the vessel was measured every 2 days during the release process. The swelling ratio of the spherical

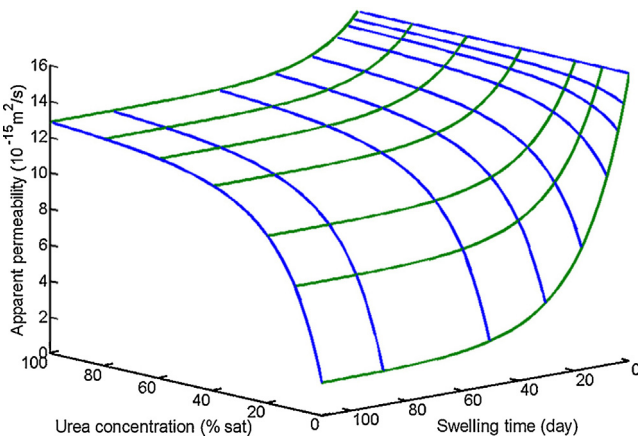


**Fig. 10.** Dependence of the apparent permeability coefficient of the planar film in urea solution on urea concentration and swelling time.

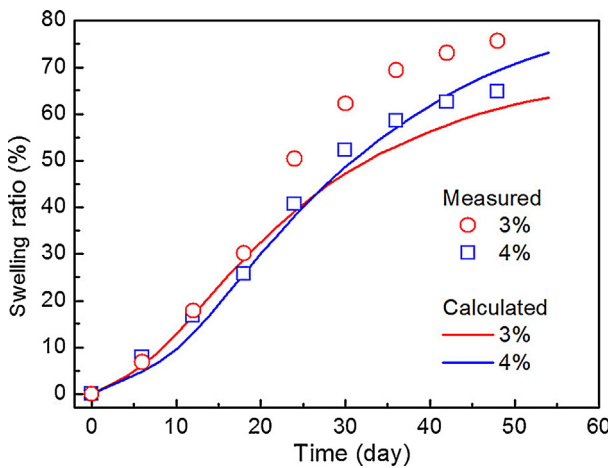


**Fig. 12.** Swelling curves of spherical films calculated from the expansion curves in Fig. 11.

film  $\Phi(C,t)$  was then obtained from the numerical solution of Eq. (16).

$$\frac{\Phi_{n+1} - \Phi_n}{\varphi_e(C) - \Phi_{n+1}} = k\Delta t, \quad (17)$$

$$\Phi_{n+1} = \frac{\Phi_n + \varphi_e(C)k\Delta t}{1 + k\Delta t}, \quad \Phi_1 = 0, \quad (18)$$

where  $\Phi_n$  is swelling ratio of the spherical film at step  $n$  in the numerical iterative process.

In the urea release process, water diffused into the particle through the film while urea was released from the particle. Early in the release process, the urea inside the film was maintained at saturation concentration until the urea dissolved completely, and then the inside urea concentration decreased during the release process. Therefore, the swelling of the spherical film during the release process was different from that of the planar film in urea solution of constant concentration. From the solutions of Eq. (18), the swelling curves of the spherical films were obtained (Fig. 12). These curves are S-shaped rather than exponential. The calculated swelling characteristics of spherical films agree reasonably with those measured. Early in the release process, the urea concentration in the particle was high, so  $\varphi$  was low. In the middle period of the release process, the inside urea concentration decreased, and  $\varphi$  increased. In the final period of the release process, although the urea concentration was low, the swelling was close to equilibrium, so  $\varphi$  changed slowly.

From Eq. (9),  $P_a$  of the spherical film was calculated,

$$P_a = \eta\Phi(C, t) + P_0. \quad (19)$$

The  $P$  values of the spherical film calculated from the swelling curves in Fig. 12 are displayed in Fig. 13 for film coating contents of 3% and 4%. Measured  $P$  are also shown in Fig. 13 for comparison. Although there were some deviations, the characteristics of the calculated  $P$  qualitatively agreed with those measured; i.e.,  $P$  decreased at first and then gradually levelled off during the release process. The deviation could be caused by the stress in the spherical film.

#### Comparison of the calculated and measured release curves

During the release process of a coated urea particle, the relationship between the surface area  $A_s(t)$  and volume  $V_s(t)$  of a spherical urea particle is

$$A_s(t) = \sqrt[3]{36\pi V_s(t)^2}. \quad (20)$$

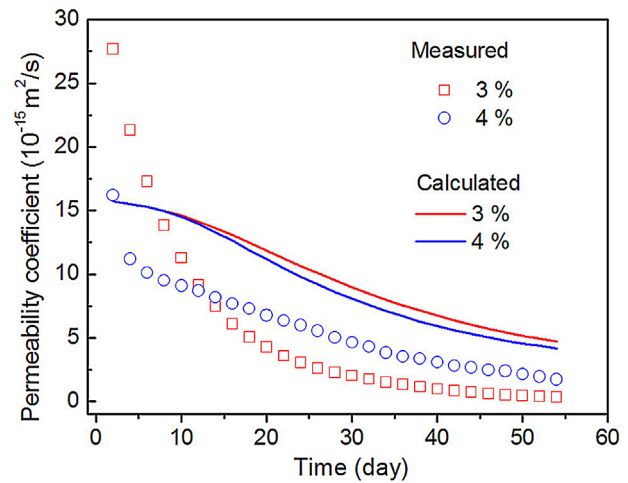


**Fig. 13.** Calculated and measured permeability coefficients of spherical films.

From the coating amount on a particle  $m_L$  and the swollen film density  $\rho$ , which is close to the density of water, the film thickness  $\delta(t)$  is

$$\delta(t) = \frac{m_L[1 + \Phi(C, t)]}{\rho A_s(t)} = \frac{m_L[1 + \Phi(C, t)]}{\rho \sqrt[3]{36\pi V_s(t)^2}}. \quad (21)$$

From  $\varphi$  of the film in the release process, we calculated  $P_a$ . By substituting the volume expansion into Eqs. (20) and (21),  $A_s(t)$  and  $\delta(t)$  were calculated. The mass of urea released in a time  $\Delta t_i$  ( $\Delta t_i = 48 \text{ h}$ ,  $i = 1, 2, \dots, n$ ) was calculated from Fick's law,

$$\Delta m_i = P_a \frac{\Delta C}{\delta} \Delta t_i A_s. \quad (22)$$

Then, the accumulated mass released from a single particle  $R_{ac}$  at  $t$  is obtained,

$$R_{ac}(\%) = \frac{1}{m_s} \sum_{i=1}^n \Delta m_i \times 100\%, \quad (23)$$

where  $m_s$  is the urea mass in a single coated urea particle. The release curves of coated urea were calculated (Fig. 14), and were similar to those measured.

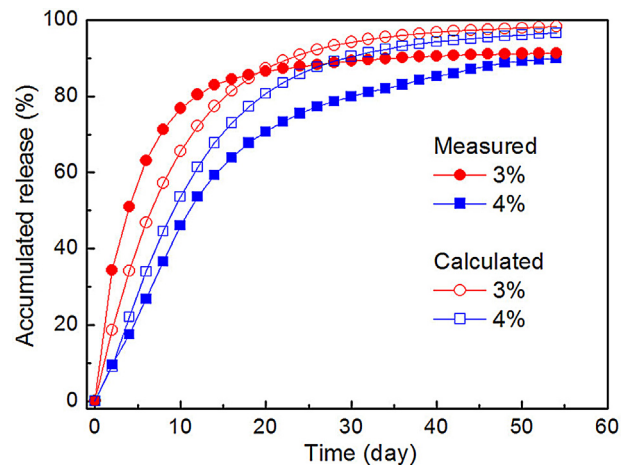


**Fig. 14.** Comparison of calculated release curves with measured ones for coated urea particles.

## Conclusions

Dense uniform latex films were coated on the surface of urea particles to control the release of urea by spray coating in a fluidized bed. The film coating formed through latex dewatering, which is a promising environmentally benign process. The coated film is hydrophilic and swells substantially in water or a moist environment. The presence of urea strongly affected film swelling. In urea solution, urea and water form hydrogen bonds, which inhibit the diffusion of water molecules and hinder the formation of hydrogen bonds between water molecules and polymer chains, limiting film swelling. The higher the urea concentration, the lower the film  $\varphi$ . The swelling kinetics in urea solution were found to be a function of urea concentration and time, with  $\varphi(C,t) = \varphi_e(C)(1 - e^{-kt})$ . Film swelling has marked effects on film structure and permeability. A higher  $\varphi$  gave a lower  $P$ , and  $P$  has an approximately linear relationship with  $\varphi$ . Based on the film formation process and swollen film structure, a model of the swollen film structure consisting of dense and swollen phases with a dot matrix distribution was proposed.  $P$  of the spherical film and the cumulative mass of urea released from the coated particles were calculated from  $\varphi$  of the spherical film, which was determined from the expansion curve of the coated particles during the release process. The calculated and measured release curves agreed well. The swelling of hydrophilic films and mechanism of controlled release are important considerations in the research and development of environmentally benign controlled-release urea.

## Acknowledgement

The authors express their gratitude for the financial support of this study by the National Natural Science Foundation of China (NSFC No. 20876085).

## References

- Alfrey, T., Gurnee, E. F., & Lloyd, W. G. (1966). Diffusion in glassy polymers. *Journal of Polymer Science-Polymer Symposia*, 12, 249–261.
- Al-Zahrani, S. M. (1999). Controlled-release of fertilizers: Modelling and simulation. *International Journal of Engineering Science*, 37, 1299–1307.
- Aranaz, I., Gutierrez, M. C., Ferrer, M. L., & del Monte, F. (2014). Preparation of chitosan nanocomposites with a macroporous structure by unidirectional freezing and subsequent freeze-drying. *Marine Drugs*, 12, 5619–5642.
- Ataman, E., & Pekcan, O. (2007). Small molecule diffusion into swelling iota-carrageenan gels: A fluorescence study. *Journal of Biomolecular Structure & Dynamics*, 24, 505–513.
- Cai, L., Liu, Y., & Liang, H. (2012). Impact of hydrogen bonding on inclusion layer of urea to cellulose: Study of molecular dynamics simulation. *Polymer*, 53, 1124–1130.
- Carr, J. K., Buchanan, L. E., Schmidt, J. R., Zanni, M. T., & Skinner, J. L. (2013). Structure and dynamics of urea/water mixtures investigated by vibrational spectroscopy and molecular dynamics simulation. *Journal of Physical Chemistry B*, 117, 13291–13300.
- Chen, J. Q., Ge, Y. M., Sun, D. F., Wang, L. P., & Zhang, M. (2012). Discussion on rapid quality detection method for slow/controlled release fertilizers. *Phosphate & Compound Fertilizer*, 5, 13–15.
- Crank, J. (1975). *The mathematics of diffusion* (2nd ed.). London: Oxford University Press.
- Dekyndt, B., Verin, J., Neut, C., Siepmann, F., & Siepmann, J. (2015). How to easily provide zero order release of freely soluble drugs from coated pellets. *International Journal of Pharmaceutics*, 478, 31–38.
- Du, C., Shen, Y., & Zhou, J. (2013). Application of aqueous silicone-acrylate emulsions in coated controlled release fertilizer. *Journal Controlled Release*, 172, E18–E19.
- Duan, L., Zhang, M., Liu, G., Yang, Y., & Shang, Z. (2009). Evaluation of nutrient release characteristics of slow and controlled-release fertilizers and fast measurement method. *Acta Pedologica Sinica*, 46, 299–307.
- Fan, L. F., He, W., Bai, M., Du, Q., Xiang, B., Chang, Y. Z., et al. (2008). Biphasic drug release: Permeability and swelling of pectin/ethylcellulose films, and in vitro and in vivo correlation of film-coated pellets in dogs. *Chemical & Pharmaceutical Bulletin*, 56, 1118–1125.
- Gambash, S., Kochba, M., & Avnimelech, Y. (1990). Studies on slow-release fertilizers. 2. A method for evaluation of nutrient release rate from slow-releasing fertilizers. *Soil Science*, 150, 446–450.
- Geissler, E., Hecht, A. M., & Duplessix, R. (1982). Comparison between neutron and quasi-elastic light-scattering by polyacrylamide gels. *Journal of Polymer Science Part B: Polymer Physics*, 20, 225–233.
- Ho, Y. S. (2004). Citation review of Lagergren kinetic rate equation on adsorption reactions. *Scientometrics*, 59, 171–177.
- Kim, E., Lee, J., Kim, D., Lee, K. E., Han, S. S., Lim, N., et al. (2009). Solvent-responsive polymer nanocapsules with controlled permeability: Encapsulation and release of a fluorescent dye by swelling and deswelling. *Chemical Communications*, 12, 1472–1474.
- Kostic, A., Adnadjevic, B., Popovic, A., & Jovanovic, J. (2007). Comparison of the swelling kinetics of a partially neutralized poly(acrylic acid) hydrogel in distilled water and physiological solution. *Journal of the Serbian Chemical Society*, 72, 1139–1153.
- Kurek, M., Guinault, A., Voilley, A., Galic, K., & Debeaufort, F. (2014). Effect of relative humidity on carvacrol release and permeation properties of chitosan based films and coatings. *Food Chemistry*, 144, 9–17.
- Lan, R. (2012). *Spray coating process and release characteristics of film coated urea by using polymer latex* (Unpublished master thesis). Beijing, China: Tsinghua University.
- Lan, R., Liu, Y., Wang, G., Wang, T., Kan, C., & Jin, Y. (2011). Experimental modeling of polymer latex spray coating for producing controlled-release urea. *Particuology*, 9, 510–516.
- Lan, R., Wang, G. D., Yang, L., Wang, T. J., Kan, C. Y., & Jin, Y. (2013). Prediction of release characteristics of film-coated urea from structure characterization data of the film. *Chemical Engineering & Technology*, 36, 347–354.
- Lang, M., John, A., & Sommer, J. U. (2016). Model simulations on network formation and swelling as obtained from cross-linking co-polymerization reactions. *Polymer*, 82, 138–155.
- Li, G., Guo, L., Meng, Y., & Zhang, T. (2011). Self-assembled nanoparticles from thermo-sensitive polyion complex micelles for controlled drug release. *Chemical Engineering Science*, 174, 199–205.
- Li, H. P., Kan, C. Y., & Liu, D. S. (2001). Effects of emulsifiers on ambient curable crosslinked acrylic-styrene emulsion. *Chemical Materials for Construction*, 3, 13–15 (in Chinese).
- Li, Y., & Tanaka, T. (1990). Kinetics of swelling and shrinking of gels. *Journal of Chemical Physics*, 92, 1365–1371.
- McCoy, J. L., & Muthukumar, M. (2010). Dynamic light scattering studies of ionic and nonionic polymer gels with continuous and discontinuous volume transitions. *Journal of Polymer Science Part B: Polymer Physics*, 48, 2193–2206.
- Rezus, Y. L. A., & Bakker, H. J. (2006). Effect of urea on the structural dynamics of water. *Proceedings of the National Academy of Sciences of the United States of America*, 103, 18417–18420.
- Schott, H. (1992). Swelling kinetics of polymers. *Journal of Macromolecular Science-Physics*, B31, 1–9.
- Shaviv, A., Raban, S., & Zaidel, E. (2003). Modeling controlled nutrient release from polymer coated fertilizers: Diffusion release from single granules. *Environmental Science & Technology*, 37, 2251–2256.
- Sivanantham, M., & Tata, B. V. R. (2012). Swelling/deswelling of polyacrylamide gels in aqueous NaCl solution: Light scattering and macroscopic swelling study. *Pramana-Journal of Physics*, 79, 457–469.
- Tanaka, T., & Fillmore, D. J. (1979). Kinetics of swelling of gels. *Journal of Chemical Physics*, 70, 1214–1218.
- Tzika, M., Alexandridou, S., & Kiparissides, C. (2003). Evaluation of the morphological and release characteristics of coated fertilizer granules produced in a Wurster fluidized bed. *Powder Technology*, 132, 16–24.
- Wang, C. J., Li, Y., & Hu, Z. B. (1997). Swelling kinetics of polymer gels. *Macromolecules*, 30, 4727–4732.
- Witono, J. R., Noordergraaf, I. W., Heeres, H. J., & Janssen, L. P. B. M. (2014). Water absorption, retention and the swelling characteristics of cassava starch grafted with polyacrylic acid. *Carbohydrate Polymers*, 103, 325–332.
- Xie, Y., Yang, X., Cao, Y., Jiang, R., & Zhang, F. (2007). Evaluation of determination methods for nutrient release characteristics of coated controlled-release fertilizer under soil and water incubation conditions. *Plant Nutrition and Fertilizer Science*, 13, 491–497.
- Yakimets, I., Paes, S. S., Wellner, N., Smith, A. C., Wilson, R. H., & Mitchell, J. R. (2007). Effect of water content on the structural reorganization and elastic properties of biopolymer films: A comparative study. *Biomacromolecules*, 8, 1710–1722.
- Yin, C., Xu, A., Gong, L., Zhang, L., Geng, B., & Zhang, S. (2015). Preparation of slightly crosslinked monodisperse poly(maleic anhydride-cyclohexyl vinyl ether-divinylbenzene) functional microspheres with anhydride groups via precipitation polymerization. *Particuology*, 19, 99–106.
- Zhu, M., & Vesely, D. (2007). The effect of polymer swelling and resistance to flow on solvent diffusion and permeability. *European Polymer Journal*, 43, 4503–4515.
- Zou, Q., Habermann-Röttinghaus, S. M., & Murphy, K. P. (1998). Urea effects on protein stability: Hydrogen bonding and the hydrophobic effect. *Proteins*, 31, 107–115.